Computers and Concrete, *Vol. 25, No. 4 (2020) 283-291*
DOI: https://doi.org/10.12989/cac.2020.25.4.283

Finite element based post-buckling analysis of refined graphene oxide reinforced concrete beams with geometrical imperfection

Seyed Sajad Mirjavadi[1], Masoud Forsat*[1], Yahya Zakariya Yahya[2], Mohammad Reza Barati[3], Anirudh Narasimamurthy Jayasimha[4] and Imran Khan[5]

[1]*Department of Mechanical and Industrial Engineering, Qatar University, P.O. Box 2713, Doha, Qatar*
[2]*Auckland Bioengineering Institute, the University of Auckland, Auckland, New Zealand*
[3]*Fidar project Qaem Company, Darvazeh Dolat, Tehran, Iran*
[4]*Bonn-Rhein-Sieg University of Applied Science, Sankt Augustin, Germany*
[5]*Department of Electrical Engineering, University of Engineering & Technology, Peshawar 814, Pakistan*

(*Received October 17, 2019, Revised February 12, 2020, Accepted February 20, 2020*)

Abstract. The present paper researches post-buckling behaviors of geometrically imperfect concrete beam resting on elastic foundation reinforced with graphene oxide powders (GOPs) based on finite element method (FEM). Distribution of GOPs are considered as uniform and linearly graded through the thickness. Geometric imperfection is considered as first buckling mode shape of the beam, the GOP reinforced beam is rested in initial position. The material properties of GOP reinforced composite have been calculated via employment of Halpin-Tsai micromechanical scheme. The provided refined beam element verifies the shear deformation impacts needless of any shear correction coefficient. The post-buckling load-deflections relations have been calculated via solving the governing equations having cubic non-linearity implementing FEM. Obtained findings indicate the importance of GOP distributions, GOP weight fraction, matrix material, geometric imperfection, shear deformation and foundation parameters on nonlinear buckling behavior of GOP reinforced beam.

Keywords: post-buckling; refined beam theory; nano-composite; graphene oxide powders; finite element method

1. Introduction

In recent decades, several carbon based structures containing carbon nanotube or carbon fiber have been widely utilized in composites for enhancing their mechanics and thermal specifications (Zhang 2017, Keleshtreri *et al*. 2016, Liew *et al*. 2020). A 273% enhancement of elastic modulus is obtained by Ahankari *et al*. (2010) for carbon reinforced composites in comparison to conventional composites. Likewise, Gojny *et al*. (2004) mentioned that structural stiffness of carbon based composites may be enhanced with incorporation of carbon nanotube within material. Impacts of configuration and scale of carbon nanotubes on rigidity growth of material composites having metallic matrices are studied by Esawi *et al*. (2011). Because of possessing above mentioned properties, beam and plate structures having carbon based fillers are researched to understand their static or dynamical status (Yang *et al*. 2017). There are also some investigations on composite or functionally graded materials and interested readers are refaced to new investigations on materials (Barati and Zenkour 2018, She *et al*. 2018, 2019, Shafiei *et al*. 2017, Mirjavadi *et al*. 2017, 2018, 2019, Azimi *et al*. 2017, 2018). Furthermore, the graphene based composite material has been recently gained enormous attentions because of having easy producing procedure and high rigidity growth. Nieto *et al*. (2017) presented a review paper based on several graphene based composite material possessing ceramic or metallic matrices. The multi-scale study of mechanical attributes for graphene based composite material has been provided by Lin *et al*. (2018) utilizing finite elements approach.

Until now, many of researches in the fields of nano-composites have been interested in production and materials characteristics recognition of graphene based composites and structural components containing slight percentages of graphene fillers. For instance, it is mentioned by Rafiee *et al*. (2009) that some material characteristics of graphene based composites may be enhanced via placing 0.1% volume of graphene filler. However, achieving to this level of reinforcement employing nanotubes required 1% of their volume. Graphene based composites containing epoxy matrix were created by King *et al*. (2013) by placing 6% weight fraction of graphene fillers to polymeric phases. It was stated that Young modulus of the composite has been increased from 2.72 GPa to 3.36 GPa. Next, 57% increment for Young modulus has been achieved by Fang *et al*. (2009) based on a sample of graphene based composite.

Moreover, many studies in the fields of nano-mechanic are associated with vibrational and stability investigation of various structural elements containing beam or plate reinforced via diverse carbon-based dispersions (Liew *et al*. 2014, Zhang and Liew 2016, Zhang *et al*. 2016a, b, c). Vibrational properties of a laminated graphene based plate have been explored by Song *et al*. (2017) assuming simply

*Corresponding author, Ph.D.
E-mail: masoudforsatlar@gmail.com

ISSN: 1598-8198 (Print), 1598-818X (Online)

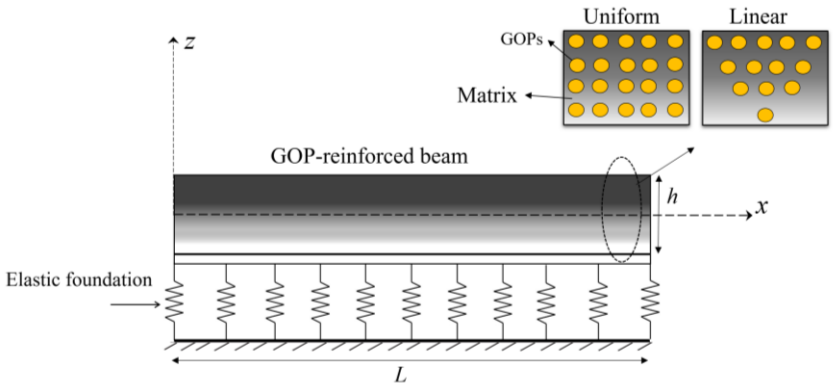

Fig. 1 A GOP-reinforced concrete beam resting on elastic foundation

support edge condition. They assumed that the plate is constructed from particular numbers of layers each containing a sensible content of graphene. Selecting a perturbation approach, static deflections and bucking loads of graphene based plates have been derived by Shen *et al*. (2017). In above papers, each material property has discontinuous variation across the thickness of beam or plate. Also, geometrically nonlinear vibration frequencies of graphene based beams having embedded graphene have been explored by Feng *et al*. (2017) selecting first-order beam theory. Moreover, vibration frequencies of graphene based beams having porosities have been explored by Kitipornchai *et al*. (2017).

Recently, reinforcement of concrete with nano-size inclusions is a novel case study. Many researches show that mechanical properties of concrete can be enhanced by adding graphene platelets (GPLs), graphene oxide powders (GOPs) and ever carbon nanotubes (Du *et al*. 2016, Shamsaei *et al*. 2018). Graphene oxide, formed from graphene, is extensively and economically accessible from graphite mass oxidation. It is compatible with many matrix materials including polymeric materials and even concrete (Mohammed *et al*. 2017). A graphene oxide composite illustrates large elastic modulus and tensile strength because it is a carbon-filled material having promising performances with a low costs (Zhang *et al*. 2020). To the best of author's knowledge, post-buckling study of geometrically imperfect concrete beams reinforced by GOPs is not performed yet.

This paper is devoted to analyze post-buckling behavior of a geometrically imperfect concrete beam reinforced with graphene oxide powders (GOPs) based on finite element method (FEM). GOPs have two types of dispersion within the structure including uniform-type and linear-type. The presented formulation is based on a higher order refined beam element accounting for shear deformations. So, it is useful for thick beams. The GOP-reinforced beam is exposed to an in-plane mechanical load leading to its buckling and is rested on elastic foundation which is modeled by two-parameter Winkler-Pasternak model. Via finite element procedure, post-buckling path of the beam has been derived. It will be demonstrated that buckling characteristics of the GOP-reinforced beam are dependent on shear deformation, geometric amplitude, GOP distribution and foundation factors.

2. GOP-based composites

According to Fig. 1, it is assumed that GOPs have two types of dispersion within the structure including uniform-type and linear-type. In this figure, a GOP reinforced composite beam is illustrated. Micro-mechanic theory of such composite materials (Liew *et al*. 2015) introduces the below relationship between GOPs weight fraction (W_{GOP}) and their volume fraction (V_{GOP}) by

$$V_{GOP}^{*}=\frac{W_{GOP}}{W_{GOP}+\frac{\rho_{GOP}}{\rho_{M}}-\frac{\rho_{GOP}}{\rho_{M}}W_{GOP}} \tag{1}$$

where ρ_{GOP} and ρ_{M} define the mass densities of GOP and matrices, respectively. Next, the elastic modulus of a GOP based composite might be represented based upon matrix elastic modulus (E_M) by (Zhang *et al*. 2020)

$$\begin{aligned}E_1=0.49&\left(\frac{1+\xi_L^{GOP}\eta_L^{GOP}V_{GOP}}{1-\eta_L^{GOP}V_{GOP}}\right)E_M\\&+0.51\left(\frac{1+\xi_W^{GOP}\eta_W^{GOP}V_{GOP}}{1-\eta_W^{GOP}V_{GOP}}\right)E_M\end{aligned} \tag{2}$$

so that ξ_L^{GOP} and ξ_W^{GOP} define two geometrical factors indicating the impacts of graphene configuration and scales as

$$\xi_L^{GOP}=\frac{2d_{GOP}}{t_{GOP}} \tag{3a}$$

$$\eta_L^{GOP}=\frac{\left(E_{GOP}/E_M\right)-1}{\left(E_{GOP}/E_M\right)+\xi_L^{GOP}} \tag{3b}$$

$$\xi_W^{GOP}=\frac{2d_{GOP}}{t_{GOP}} \tag{3c}$$

$$\eta_W^{GOP}=\frac{\left(E_{GOP}/E_M\right)-1}{\left(E_{GOP}/E_M\right)+\xi_W^{GOP}} \tag{3d}$$

so that d_{GPL} and t_{GPL} define GOP average diameter and thickness, respectively. Furthermore, Poisson's ratio for GOP based composite might be defined based upon Poisson's ratio of the two constituents in the form

$$\nu_1=\nu_{GOP}V_{GOP}+\nu_M V_M \tag{4}$$

in which V_M=1−V_{GOP} expresses the volume fractions of matrix component. Herein, two dispersions of the GOP have been assumed as:

Uniform:

$$V_{GOP} = V_{GOP}^{*} \tag{5}$$

Linear:

$$V_{GOP} = (1+2\frac{z}{h})V_{GOP}^{*} \tag{6}$$

3. Beam modeling via refined theory

So far, a variety of beam theories are introduced for description and analyzes of beam structures (Barati 2017, Fenjan *et al*. 2019, Ahmed *et al*. 2019, Abualnour *et al*. 2019, Adda Bedia *et al*. 2019, Alimirzaei *et al*. 2019, Batou *et al*. 2019, Belbachir *et al*. 2019, Berghouti *et al*. 2019, Boukhlif *et al*. 2019, Bourada *et al*. 2019, Boutaleb *et al*. 2019, Boulefrakh *et al*. 2019, Chaabane *et al*. 2019, Draoui *et al*. 2019, Hellal *et al*. 2019, Hussain *et al*. 2019, Kaddari *et al*. 2020, Khiloun *et al*. 2019, Mahmoudi *et al*. 2019, Medani *et al*. 2019, Meksi *et al*. 2019, Sahla *et al*. 2019, Semmah *et al*. 2019, Tlidji *et al*. 2019, Zarga *et al*. 2019, Zaoui *et al*. 2019). The displacement field containing axial displacement (u_1) and transverse displacement (u_3) with respect to the refined beam assumption calculating the precise location of the neutral axis might be defined as (Draiche *et al*. 2019, Addou *et al*. 2019)

$$u_1(x,z) = u(x) - (z-z^{*})\frac{\partial w_b}{\partial x} - [f(z)-z^{**}]\frac{\partial w_s}{\partial x} \tag{7}$$

$$u_3(x,z) = w(x) = w_b(x) + w_s(x) \tag{8}$$

where the present theory has a third-order function in the form

$$f(z) = -\frac{z}{4} + \frac{5z^3}{3h^2} \tag{9}$$

and

$$z^{*} = \frac{\int_{-h/2}^{h/2} E(z)\, z dz}{\int_{-h/2}^{h/2} E(z)\, dz}, \quad z^{**} = \frac{\int_{-h/2}^{h/2} E(z)\, f(z) dz}{\int_{-h/2}^{h/2} E(z)\, dz} \tag{10}$$

Above displacement field is calculated form the axial displacement (u), together with w_b and w_s as bending and shear displacements. Accordingly, one may calculate the strains of as (Ahmed *et al*. 2019)

$$\begin{aligned} \varepsilon_x &= \frac{\partial u}{\partial x} + \frac{1}{2}(\frac{\partial w}{\partial x})^2 - (z-z^{*})\frac{\partial^2 w_b}{\partial x^2} - [f(z)-z^{**}]\frac{\partial^2 w_s}{\partial x^2} \\ \gamma_{xz} &= g(z)\frac{\partial w_s}{\partial x} \end{aligned} \tag{11}$$

Based on proposed beam model and using Hamilton's rule, one can express the governing equations of the GOP reinforced beam as follows (Ahmed *et al*. 2019)

$$\frac{\partial N_x}{\partial x} = 0 \tag{12}$$

$$\begin{aligned} &\frac{\partial^2 M_x^b}{\partial x^2} + \frac{\partial}{\partial x}(N_x \frac{\partial (w_b+w_s)}{\partial x}) = +k_L(w_b+w_s) \\ &-k_P\nabla^2(w_b+w_s) + k_{NL}(w_b+w_s)^3 = 0 \end{aligned} \tag{13}$$

$$\begin{aligned} &\frac{\partial^2 M_x^s}{\partial x^2} + \frac{\partial Q_{xz}}{\partial x} + \frac{\partial}{\partial x}(N_x \frac{\partial (w_b+w_s)}{\partial x}) - k_L(w_b+w_s) \\ &+k_P\nabla^2(w_b+w_s) - k_{NL}(w_b+w_s)^3 = 0 \end{aligned} \tag{14}$$

So that forces and moments might be calculated as (Faleh *et al*. 2018, She *et al*. 2018)

$$\begin{aligned} &(N_x, M_x^b, M_x^s) = \int_{-h/2}^{h/2} (1, z-z^{*}, f-z^{**})\sigma_x\, dz, \\ &Q_{xz} = \int_{-h/2}^{h/2} g(z)\sigma_{xz} dz \end{aligned} \tag{15}$$

Also, k_L, k_P, and k_{NL} defines linear, shear and non-linear types of foundation.

Taking into account geometric imperfection effect and with aid of Eq. (15), the relations for force-strain and the moment-strain might be derived

$$N_x = A[\frac{\partial u}{\partial x} + \frac{1}{2}(\frac{\partial (w_b+w_s)}{\partial x})^2 - \frac{1}{2}(\frac{\partial (w_b^{*}+w_s^{*})}{\partial x})^2] \tag{16}$$

$$M_x^b = -D(\frac{\partial^2 w_b}{\partial x^2} - \frac{\partial^2 w_b^{*}}{\partial x^2}) - E(\frac{\partial^2 w_s}{\partial x^2} - \frac{\partial^2 w_s^{*}}{\partial x^2}) \tag{17}$$

$$M_x^s = -E(\frac{\partial^2 w_b}{\partial x^2} - \frac{\partial^2 w_b^{*}}{\partial x^2}) - F(\frac{\partial^2 w_s}{\partial x^2} - \frac{\partial^2 w_s^{*}}{\partial x^2}) \tag{18}$$

$$Q_{xz} = A_s \frac{\partial w_s}{\partial x} \tag{19}$$

in which

$$\begin{aligned} &A = \int_{-h/2}^{h/2} E(z)\, dz, \;\; D = \int_{-h/2}^{h/2} E(z)(z-z^{*})^2\, dz, \\ &E = \int_{-h/2}^{h/2} E(z)(z-z^{*})(f-z^{**})\, dz \\ &F = \int_{-h/2}^{h/2} E(z)(f-z^{**})^2\, dz, \quad A_s = \int_{-h/2}^{h/2} \frac{E(z)}{2(1+\nu)} g^2 dz \end{aligned} \tag{20}$$

There are three nonlinear governing equations for proposed refined beam model which can be written with respect to displacements from inserting Eqs. (16)-(19), into Eqs. (12)-(14) as

$$\begin{aligned} &A(\frac{\partial^2 u}{\partial x^2}) + A(\frac{\partial (w_b+w_s)}{\partial x}\frac{\partial^2 (w_b+w_s)}{\partial x^2} \\ &+\frac{\partial (w_b^{*}+w_s^{*})}{\partial x}\frac{\partial^2 (w_b^{*}+w_s^{*})}{\partial x^2}) = 0 \end{aligned} \tag{21}$$

$$\begin{aligned} &-D(\frac{\partial^4 w_b}{\partial x^4} - \frac{\partial^4 w_b^{*}}{\partial x^4}) - E(\frac{\partial^4 w_s}{\partial x^4} - \frac{\partial^4 w_s^{*}}{\partial x^4}) \\ &+\frac{\partial}{\partial x}(N_x \frac{\partial w}{\partial x}) - k_L(w_b+w_s-w_b^{*}-w_s^{*}) \\ &+k_P(\frac{\partial^2 w_b}{\partial x^2} - \frac{\partial^2 w_b^{*}}{\partial x^2} + \frac{\partial^2 w_s}{\partial x^2} - \frac{\partial^2 w_s^{*}}{\partial x^2}) \\ &-k_{NL}[(w_b+w_s)^3 - (w_b^{*}+w_s^{*})^3] = 0 \end{aligned} \tag{22}$$

$$-E(\frac{\partial^4 w_b}{\partial x^4} - \frac{\partial^4 w_b^{*}}{\partial x^4}) - F(\frac{\partial^4 w_s}{\partial x^4} - \frac{\partial^4 w_s^{*}}{\partial x^4})$$

$$+\frac{\partial}{\partial x}(N_x\frac{\partial w}{\partial x})+A_{44}(\frac{\partial^2 w_s}{\partial x^2}-\frac{\partial^2 w_s^*}{\partial x^2})$$
$$-k_L(w_b+w_s-w_b^*-w_s^*)$$
$$+k_P(\frac{\partial^2 w_b}{\partial x^2}-\frac{\partial^2 w_b^*}{\partial x^2}+\frac{\partial^2 w_s}{\partial x^2}-\frac{\partial^2 w_s^*}{\partial x^2})$$
$$-k_{NL}[(w_b+w_s)^3-(w_b^*+w_s^*)^3]=0 \quad (23)$$

It is proved that the first derivative of axial displacement (u) based on $u(0)=0$, $u(L)=-PL/A$ can be calculated as (Ahmed *et al*. 2019)

$$\frac{\partial u}{\partial x}=-\frac{1}{2}(\frac{\partial(w_b+w_s)}{\partial x})^2+\frac{1}{2}(\frac{\partial(w_b^*+w_s^*)}{\partial x})^2$$
$$+\frac{1}{2L}\int_0^L(\frac{\partial(w_b+w_s)}{\partial x})^2dx-\frac{1}{2L}\int_0^L(\frac{\partial(w_b^*+w_s^*)}{\partial x})^2dx-\frac{P}{A} \quad (24)$$

where P is applied in-pane mechanical load. The above expression can be place into the governing equations in order to eliminating axial displacement.

4. Solution by FEM

Through the present section, FEM has been selected for solving the buckling problem of a GOP based beam with geometric imperfection. For this goal, the refined beam element has been used with ten degrees of freedom. Herein, a shape function has been introduced for axial field component, and also Hermit shape function have been introduced for lateral field components which are

$$u(x)=\sum_{i=1}^{2}U_iN_i(x)=N_1U_1+N_2U_2 \quad (25)$$

$$w_b(x)=\sum_{i=1}^{4}a_i\tilde{N}_i(x)=\tilde{N}_1W_{b1}+\tilde{N}_2W'_{b2}+\tilde{N}_3W_{b3}+\tilde{N}_4W'_{b4} \quad (26)$$

$$w_s(x)=\sum_{i=1}^{4}b_i\tilde{N}_i(x)=\tilde{N}_1W_{s1}+\tilde{N}_2W'_{s2}+\tilde{N}_3W_{s3}+\tilde{N}_4W'_{s4} \quad (27)$$

So that U_i , a_i and b_i are field coefficients. Also, $a_i=\{W_{b1},W'_{b2},W_{b3},W'_{b4}\}$ and $b_i=\{W_{s1},W'_{s2},W_{s3},W'_{s4}\}$ and shape functions are

$$N_1=1-\frac{x}{L_e} \quad (28)$$

$$N_2=\frac{x}{L_e} \quad (29)$$

$$\tilde{N}_1=\frac{1}{L_e^3}\left(2x^3-3x^2L_e+L_e^3\right) \quad (30)$$

$$\tilde{N}_2=\frac{1}{L_e^3}\left(x^3L_e-2x^2L_e^2+xL_e^3\right) \quad (31)$$

$$\tilde{N}_3=\frac{1}{L_e^3}\left(-2x^3+3x^2L_e\right) \quad (32)$$

$$\tilde{N}_4=\frac{1}{L_e^3}\left(x^3L_e-x^2L_e^2\right) \quad (33)$$

so that L_e defines the length for master element.

Placing Eqs. (21)-(23) in Hamiltonian (H) and minimizing it to field coefficients U_i, W_{bi}, and W_{si} (Rezaiee-Pajand *et al*. 2018, Al-Maliki *et al*. 2019) results in below relation containing simultaneous algebraic equations

$$\frac{\partial H}{\partial U_i}=\frac{\partial H}{\partial W_{bi}}=\frac{\partial H}{\partial W_{si}}=0 \quad (34)$$

Then, by considering Eq. (24) two coupled nonlinear governing equation will be derived

$$k_{1,1}W_b+k_{1,2}W_s+G^*\tilde{W}^3+\Psi_{1,1}W_b^*+\Psi_{1,2}W_s^*=0 \quad (35)$$

$$k_{2,1}W_b+k_{2,2}W_s+G^*\tilde{W}^3+\Psi_{2,1}W_b^*+\Psi_{2,2}W_s^*=0 \quad (36)$$

in which $\tilde{W}=W_b+W_s$ is such a way that W_b and W_s are amximuum values of beanding and shear deflections, respectively and W_b^* and W_s^* are magnitude of imperfection due to initial bending and shear deflections, respectively. Also, $k_{i,j}$ and $\Psi_{i,j}$ define linear stiffness matrix respectively for perfect and imperfect master element. Also, G^* is the nonlinear stiffness matrix of master element. Simultaneously solving the two equation for finding buckling load will give the post-buckling path of the beam. Here, calculations have been carried out according to below dimensionless factors

$$K_L=\mathrm{k}_L\frac{\mathrm{L}^4}{D},\ K_p=\mathrm{k}_p\frac{\mathrm{L}^2}{D},$$
$$K_{NL}=\mathrm{k}_{NL}\frac{\mathrm{L}^4}{A},\tilde{P}=P\frac{12\mathrm{L}^2}{E_mh^3} \quad (37)$$

5. Discussions and results

According to the section, new findings have been presented for post-buckling investigation of GOP reinforced concrete beams modeled as a refined thick structure incorporating geometric imperfectness. Before all, the critical buckling loads of GOP reinforced beams have been verified by using the data of Timoshenko beams reported by Zhang *et al*. (2020), as presented in Table 1. To do this, a S-S beam having uniform distribution of GOPs is selected. With respect to different of slenderness ratio (L/h), an excellent agreement is achieved among obtained critical buckling loads with those provided by Zhang *et al*. (2020). In the present study, the material properties of GOP reinforced beam with concrete matrix are selected as:

- E_{GOP}=444.8 GPa, d_{GOP}=500 nm, t_{GOP}=0.95 nm, v_{GOP}=0.165.
- E_M=16.9 GPa, v_M=0.15.

Table 1 Validation of critical buckling load for a GOP-reinforced beam with epoxy matrix

W_{GOP}		Zhang *et al*. (2020)	Present FEM solution
0.3%	L/h=10	0.0101	0.0101
	L/h=15	0.0046	0.0047
	L/h=20	0.0026	0.0027

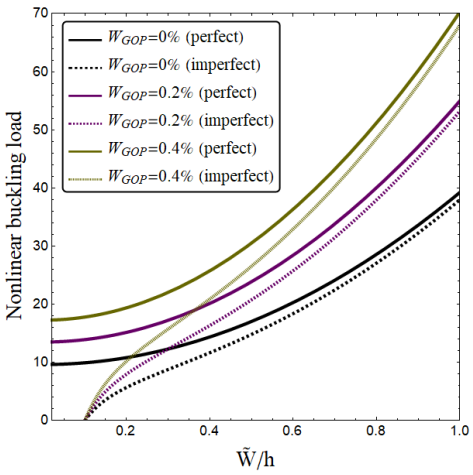

Fig. 2 Post-buckling load of perfect and imperfect beams versus dimensionless deflection for different GOP weight fractions (L/h=10, K_L=K_P=K_{NL}=0, W^*/h=0.1)

GOP amount effects on the post-buckling characteristics of concrete beams is presented in Fig. 2 at imperfection amplitude of W^*/h=0.1. Uniform GOP distribution has been considered. For an ideal (perfect) GOP-reinforced beam, the starting point ($\widetilde{W}/h = 0$) is critical buckling load. But, for an imperfect GOP-reinforced beam ($\widetilde{W}/h \neq 0$), there is no critical buckling load, since the beam is at its initial configuration. It is well-known that the nonlinear buckling load gets larger with the increase of non-dimension amplitude. This is due to the intrinsic stiffening effect. Reinforcing effect of GOPs on mechanical behavior of the beam is clearly observable in this figure. Indeed, the total stiffness of the reinforced concrete beam may be substantially strengthened by including a slight amount of GOPs in matrix material (concrete). Hereupon, non-linear stability load magnifies by the growth of GOP weight fraction (W_{GOP}).

In Fig. 3, post-buckling load-amplitude curves of a GOP-reinforced concrete beam with and without geometric imperfections have been presented accounting for various GOP weight fraction and dispersions. It is considered that L/h=10 and W^*=0.02h. The most important observation from this figure is that increasing GOP weight fraction yields larger buckling loads for all types of GOP distributions. It means that adding the amount of GOP can increase the beam stiffness and enhance its post-buckling behavior. Moreover, uniform GOP distribution provides greater post-buckling loads than linear distribution. This is due to larger amount of GOP at the upper surface of nano-composite beam. As a conclusion, control of GOP is crucial to obtain the best mechanical performance for concrete beams.

Shear deformation effect on post-buckling behavior of concrete GOP-reinforced beam has been plotted in Fig. 4 via comparison of obtained results for classic and refined higher-order beam models. Geometric imperfection amplitude is selected as W^*/h=0.02. This figure shows that refined beam model gives lower post-buckling loads than classic beam theory due to incorporating shear deformation effect. So, the presented refined beam formulation is more accurate for post-buckling analysis of thick concrete GOP-reinforced beams.

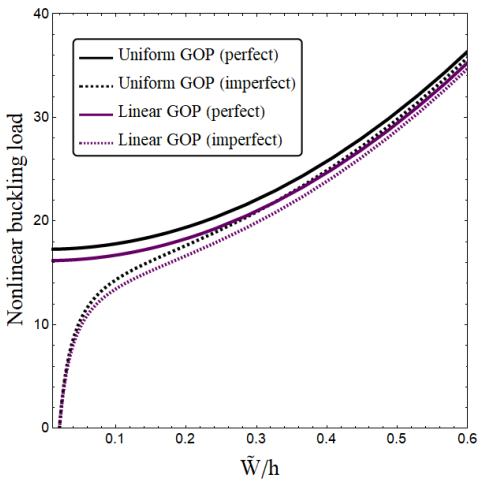

(a) W_{GOP}=0.4%

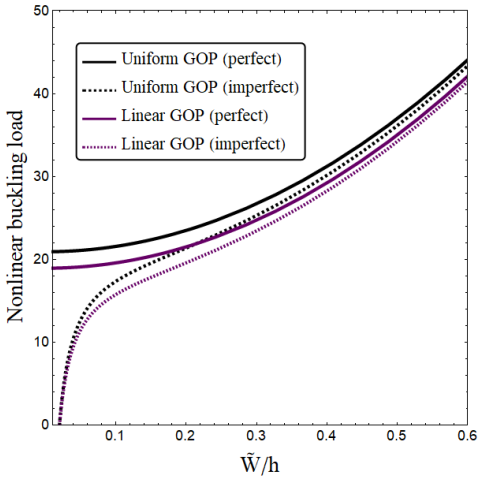

(b) W_{GOP}=0.6%

Fig. 3 Post-buckling load of perfect and imperfect beam versus dimensionless deflection for different GOP distributions (L/h=10, K_L=K_P=K_{NL}=0, W^*/h=0.02)

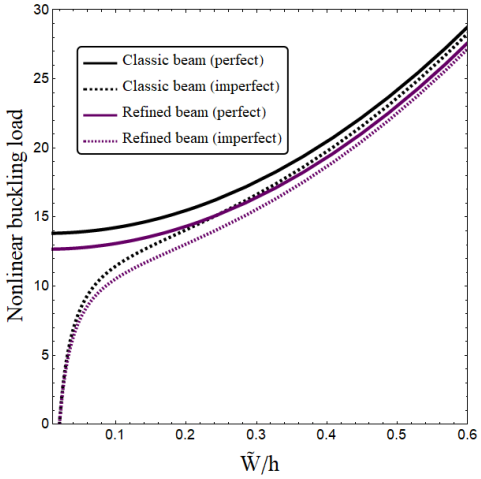

Fig. 4 Post-buckling load of perfect and imperfect porous beam versus dimensionless deflection for different beam models (L/h=5, K_L=K_P=K_{NL}=0, W_{GOP}=0.2 %, W^*/h=0.02)

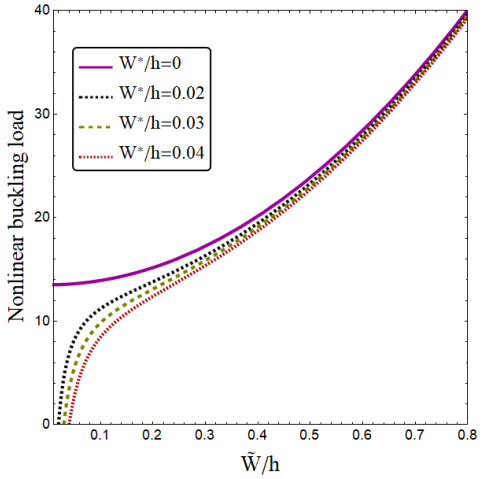

Fig. 5 Post-buckling load of porous beam with uniform GOPs versus dimensionless deflection for different geometric imperfections (L/h=10, K_L=K_P=K_{NL}=0, W_{GOP}=0.2%)

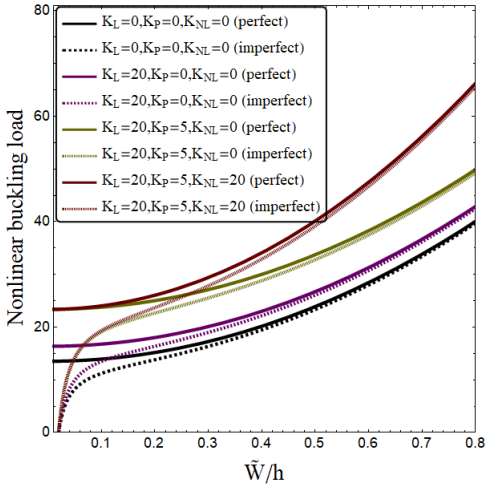

Fig. 6 Post-buckling load of the beam with uniform GOPs versus dimensionless deflection for different foundation parameters (L/h=10, W_{GOP}=0.2 %)

Geometric imperfectness (W^*/h) effects on post-buckling behaviors of GOP-reinforced beams are depicted in Fig. 5 selecting W_{GOP}=0.2%. An important fact is that the initial deflection of GOP-reinforced beam has huge influences on non-linear load-deflection path. According to before discussions, the critical buckling load vanishes by considering the primary geometric imperfectness. Indeed, considering perfect configurations (W^*/h=0) results in critical buckling of the GOP-reinforced beam. Next, beam buckling capacity improves with the growth of non-dimension amplitudes. However, considering imperfect configurations ($W^*/h\neq0$), results in no buckling capacity before the primary condition of the GOP-reinforced beam. An important finding is that as the magnitude of imperfection is greater, the post-buckling load is lower.

Fig. 6 indicates the variations of non-linear buckling load of a GOP-reinforced beam against non-dimension amplitudes with respect to diverse linear (K_L), shear (K_P) and non-linear (K_{NL}) foundation factors when W_{GOP}=0.2%.

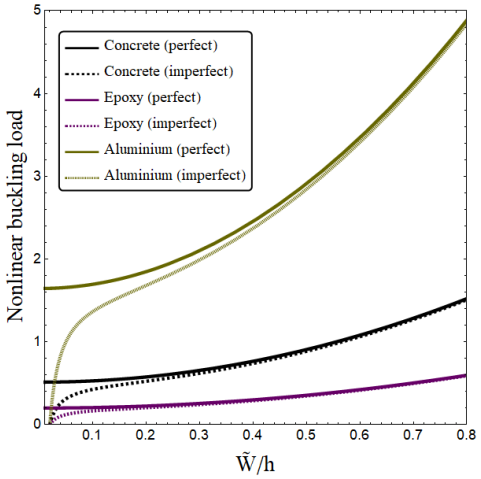

Fig. 7 Post-buckling load of beam with uniform GOPs versus dimensionless deflection for different matrix materials (L/h=10, W_{GOP}=0.2 %)

An important fact is that K_P prepares a joined interplay with the GOP-reinforced beam, whereas K_L prepares a halting interplay with the beam. Augmenting foundation factors produces greater non-linear stability loads by elevating the transverse strength of the GOP-reinforced beam. A significant fact is that the impacts of non-linear foundation factor on non-linear buckling are remarkably influenced by the geometric non-linearity or non-dimension amplitudes, whereas the impacts of K_L and K_P on buckling load are not influenced by the geometric non-linearity. Indeed, as the non-dimension amplitudes become greater, the impacts of K_{NL} on non-linear buckling load gets more announced.

Fig. 7 illustrates the effect of matrix material on post-buckling curves of the beam at a prescribed amount of GOPs (W_{GOP}=0.2%). Three types of material including concrete, epoxy (E=3.5 GPa) and Aluminum (E=70 GPa) are considered as matrix material. The maximum and minimum values of normalized buckling loads ($\tilde{P} = 12L^2P/E_{GOP}h^3$) are obtained for Aluminum and epoxy matrices. Actually, epoxy matrix gives smaller post-buckling loads than concrete matrix due to having lower stiffness. Accordingly, type of matrix material has a key role on post-buckling behavior of perfect/imperfect GOP-reinforced beams.

6. Conclusions

The present paper researched post-buckling behaviors of geometrically imperfect concrete beam resting on elastic foundation reinforced with graphene oxide powders (GOPs) based on finite element method (FEM). Distribution of GOPs were considered as uniform and linearly graded through the thickness. Geometric imperfection was considered as first buckling mode shape of the beam, so the GOP reinforced beam is rested in initial position. The most important observation was that increasing GOP weight fraction yields larger buckling loads for all types of GOP distributions. It means that adding the amount of GOP can increase the beam stiffness and enhance its post-buckling

behavior. Moreover, uniform GOP distribution provided greater post-buckling loads than linear distribution. This is due to larger amount of GOP at the upper surface of nano-composite beam. Also, it was found that refined beam model gives lower post-buckling loads than classic beam theory due to incorporating shear deformation effect. An important finding was that as the magnitude of imperfection is greater, the post-buckling load is lower.

References

Abualnour, M., Chikh, A., Hebali, H., Kaci, A., Tounsi, A., Bousahla, A.A. and Tounsi, A. (2019), "Thermomechanical analysis of antisymmetric laminated reinforced composite plates using a new four variable trigonometric refined plate theory", *Comput. Concrete*, **24**(6), 489-498. https://doi.org/10.12989/cac.2019.24.6.489.

Addou, F.Y., Meradjah, M., Bousahla, A.A., Benachour, A., Bourada, F., Tounsi, A. and Mahmoud, S.R. (2019), "Influences of porosity on dynamic response of FG plates resting on Winkler/Pasternak/Kerr foundation using quasi 3D HSDT", *Comput. Concrete*, **24**(4), 347-367. https://doi.org/10.12989/cac.2019.24.4.347.

Ahankari, S.S and Kar, K.K. (2010), "Hysteresis measurements and dynamic mechanical characterization of functionally graded natural rubber-carbon black composites", *Polym. Eng. Sci.*, **50**(5), 871-877. https://doi.org/10.1002/pen.21601.

Ahmed, R.A., Fenjan, R.M. and Faleh, N.M. (2019), "Analyzing post-buckling behavior of continuously graded FG nanobeams with geometrical imperfections", *Geomech. Eng.*, **17**(2), 175-180. https://doi.org/10.12989/gae.2019.17.2.175.

Al-Maliki, A.F., Faleh, N.M. and Alasadi, A.A. (2019), "Finite element formulation and vibration of nonlocal refined metal foam beams with symmetric and non-symmetric porosities", *Struct. Monit. Mainten.*, **6**(2), 147-159. https://doi.org/10.12989/smm.2019.6.2.147.

Alimirzaei, S., Mohammadimehr, M. and Tounsi, A. (2019), "Nonlinear analysis of viscoelastic micro-composite beam with geometrical imperfection using FEM: MSGT electro-magneto-elastic bending, buckling and vibration solutions", *Struct. Eng. Mech.*, **71**(5), 485-502. https://doi.org/10.12989/sem.2019.71.5.485.

Azimi, M., Mirjavadi, S.S., Shafiei, N. and Hamouda, A.M.S. (2017), "Thermo-mechanical vibration of rotating axially functionally graded nonlocal Timoshenko beam", *Appl. Phys. A*, **123**(1), 104. https://doi.org/10.1007/s00339-016-0712-5.

Azimi, M., Mirjavadi, S.S., Shafiei, N., Hamouda, A.M.S. and Davari, E. (2018), "Vibration of rotating functionally graded Timoshenko nano-beams with nonlinear thermal distribution", *Mech. Adv. Mater. Struct.*, **25**(6), 467-480. https://doi.org/10.1080/15376494.2017.1285455.

Balubaid, M., Tounsi, A., Dakhel, B. and Mahmoud, S.R. (2019), "Free vibration investigation of FG nanoscale plate using nonlocal two variables integral refined plate theory", *Comput. Concrete*, **24**(6), 579-586. https://doi.org/10.12989/cac.2019.24.6.579.

Barati, M.R. (2017), "Nonlocal-strain gradient forced vibration analysis of metal foam nanoplates with uniform and graded porosities", *Adv. Nano Res.*, **5**(4), 393-414. https://doi.org/10.12989/anr.2017.5.4.393.

Barati, M.R. and Zenkour, A.M. (2018), "Analysis of postbuckling of graded porous GPL-reinforced beams with geometrical imperfection", *Mech. Adv. Mater. Struct.*, **26**(6), 503-511. https://doi.org/10.1080/15376494.2017.1400622.

Batou, B., Nebab, M., Bennai, R., Atmane, H.A., Tounsi, A. and Bouremana, M. (2019), "Wave dispersion properties in imperfect sigmoid plates using various HSDTs", *Steel Compos. Struct.*, **33**(5), 699. https://doi.org/10.12989/scs.2019.33.5.699.

Bedia, W.A., Houari, M.S.A., Bessaim, A., Bousahla, A.A., Tounsi, A., Saeed, T. and Alhodaly, M.S. (2019), "A new hyperbolic two-unknown beam model for bending and buckling analysis of a nonlocal strain gradient nanobeams", *J. Nano Res.*, **57**, 175-191. https://doi.org/10.4028/www.scientific.net/JNanoR.57.175.

Belbachir, N., Draich, K., Bousahla, A.A., Bourada, M., Tounsi, A. and Mohammadimehr, M. (2019), "Bending analysis of anti-symmetric cross-ply laminated plates under nonlinear thermal and mechanical loadings", *Steel Compos. Struct.*, **33**(1), 913-924. https://doi.org/10.12989/scs.2019.33.1.081.

Berghouti, H., Adda Bedia, E.A., Benkhedda, A. and Tounsi, A. (2019), "Vibration analysis of nonlocal porous nanobeams made of functionally graded material", *Adv. Nano Res.*, **7**(5), 351-364. https://doi.org/10.12989/anr.2019.7.5.351.

Boukhlif, Z., Bouremana, M., Bourada, F., Bousahla, A.A., Bourada, M., Tounsi, A. and Al-Osta, M.A. (2019), "A simple quasi-3D HSDT for the dynamics analysis of FG thick plate on elastic foundation", *Steel Compos. Struct.*, **31**(5), 503-516. https://doi.org/10.12989/scs.2019.31.5.503.

Boulefrakh, L., Hebali, H., Chikh, A., Bousahla, A.A., Tounsi, A. and Mahmoud, S.R. (2019), "The effect of parameters of visco-Pasternak foundation on the bending and vibration properties of a thick FG plate", *Geomech. Eng.*, **18**(2), 161-178. https://doi.org/10.12989/gae.2019.18.2.161.

Bourada, F., Bousahla, A.A., Bourada, M., Azzaz, A., Zinata, A. and Tounsi, A. (2019), "Dynamic investigation of porous functionally graded beam using a sinusoidal shear deformation theory", *Wind Struct.*, **28**(1), 19-30. https://doi.org/10.12989/was.2019.28.1.019.

Boutaleb, S., Benrahou, K H., Bakora, A., Algarni, A., Bousahla, A.A., Tounsi, A., ... & Mahmoud, S.R. (2019), "Dynamic analysis of nanosize FG rectangular plates based on simple nonlocal quasi 3D HSDT", *Adv. Nano Res.*, **7**(3), 189-206. https://doi.org/10.12989/anr.2019.7.3.191.

Chaabane, L.A., Bourada, F., Sekkal, M., Zerouati, S., Zaoui, F. Z., Tounsi, A., ... & Tounsi, A. (2019), "Analytical study of bending and free vibration responses of functionally graded beams resting on elastic foundation", *Struct. Eng. Mech.*, **71**(2), 185-196. https://doi.org/10.12989/sem.2019.71.2.185.

Draiche, K., Bousahla, A.A., Tounsi, A., Alwabli, A.S., Tounsi, A. and Mahmoud, S.R. (2019), "Static analysis of laminated reinforced composite plates using a simple first-order shear deformation theory", *Comput. Concrete*, **24**(4), 369-378. https://doi.org/10.12989/cac.2019.24.4.369.

Draoui, A., Zidour, M., Tounsi, A. and Adim, B. (2019), "Static and dynamic behavior of nanotubes-reinforced sandwich plates using (FSDT)", *Adv. Nano Res.*, **57**, 117-135. https://doi.org/10.4028/www.scientific.net/JNanoR.57.117.

Du, H., Gao, H.J. and Dai Pang, S. (2016), "Improvement in concrete resistance against water and chloride ingress by adding graphene nanoplatelet", *Cement Concrete Res.*, **83**, 114-123. https://doi.org/10.1016/j.cemconres.2016.02.005.

Esawi, A.M.K., Morsi, K., Sayed, A., Taher, M and Lanka, S. (2011), "The influence of carbon nanotube (CNT) morphology and diameter on the processing and properties of CNT-reinforced aluminium composites", *Compos. Part A: Appl. Sci. Manuf.*, **42**(3), 234-243. https://doi.org/10.1016/j.compositesa.2010.11.008.

Faleh, N.M., Ahmed, R.A. and Fenjan, R.M. (2018), "On vibrations of porous FG nanoshells", *Int. J. Eng. Sci.*, **133**, 1-14. https://doi.org/10.1016/j.ijengsci.2018.08.007.

Fang, M., Wang, K., Lu, H., Yang, Y. and Nutt, S. (2009). Covalent polymer functionalization of graphene nanosheets and mechanical properties of composites", *J. Mater. Chem.*, **19**(38), 7098-7105. https://doi.org/10.1039/B908220D.

Feng, C., Kitipornchai, S. and Yang, J. (2017). Nonlinear free vibration of functionally graded polymer composite beams reinforced with graphene nanoplatelets (GPLs)", *Eng. Struct.*, **140**, 110-119. https://doi.org/10.1016/j.engstruct.2017.02.052.

Fenjan, R.M., Ahmed, R.A., Alasadi, A.A. and Faleh, N.M. (2019), "Nonlocal strain gradient thermal vibration analysis of double-coupled metal foam plate system with uniform and non-uniform porosities", *Coupl. Syst. Mech.*, **8**(3), 247-257. https://doi.org/10.12989/csm.2019.8.3.247.

Gojny, F.H., Wichmann, M.H.G., Köpke, U., Fiedler, B and Schulte, K. (2004), "Carbon nanotube-reinforced epoxy-composites: enhanced stiffness and fracture toughness at low nanotube content", *Compos. Sci. Technol.*, **64**(15), 2363-2371. https://doi.org/10.1016/j.compscitech.2004.04.002.

Hellal, H., Bourada, M., Hebali, H., Bourada, F., Tounsi, A., Bousahla, A.A. and Mahmoud, S.R. (2019), "Dynamic and stability analysis of functionally graded material sandwich plates in hygro-thermal environment using a simple higher shear deformation theory", *J. Sandw. Struct. Mater.*, 1099636219845841. https://doi.org/10.1177/1099636219845841.

Hussain, M., Naeem, M.N., Tounsi, A. and Taj, M. (2019), "Nonlocal effect on the vibration of armchair and zigzag SWCNTs with bending rigidity", *Adv. Nano Res.*, **7**(6), 431-442. https://doi.org/10.12989/anr.2019.7.6.431.

Kaddari, M., Kaci, A., Bousahla, A.A., Tounsi, A., Bourada, F., Bedia, E.A. and Al-Osta, M.A. (2020), "A study on the structural behaviour of functionally graded porous plates on elastic foundation using a new quasi-3D model: Bending and Free vibration analysis", *Comput. Concrete*, **25**(1), 37-57. https://doi.org/10.12989/cac.2020.25.1.037.

Keleshteri, M.M., Asadi, H. and Wang, Q. (2017), "Large amplitude vibration of FG-CNT reinforced composite annular plates with integrated piezoelectric layers on elastic foundation", *Thin Wall. Struct.*, **120**, 203-214. https://doi.org/10.1016/j.tws.2017.08.035.

Khiloun, M., Bousahla, A.A., Kaci, A., Bessaim, A., Tounsi, A. and Mahmoud, S.R. (2019), "Analytical modeling of bending and vibration of thick advanced composite plates using a four-variable quasi 3D HSDT", *Eng. Comput.*, 1-15. https://doi.org/10.1007/s00366-019-00732-1.

King, J.A., Klimek, D.R., Miskioglu, I. and Odegard, G.M. (2013), "Mechanical properties of graphene nanoplatelet/epoxy composites", *J. Appl. Polym. Sci.*, **128**(6), 4217-4223. https://doi.org/10.1002/app.38645.

Kitipornchai, S., Chen, D. and Yang, J. (2017), "Free vibration and elastic buckling of functionally graded porous beams reinforced by graphene platelets", *Mater. Des.*, **116**, 656-665. https://doi.org/10.1016/j.matdes.2016.12.061.

Lal, A. and Markad, K. (2018), "Deflection and stress behaviour of multi-walled carbon nanotube reinforced laminated composite beams", *Comput. Concrete*, **22**(6), 501-514. https://doi.org/10.12989/cac.2018.22.6.501.

Liew, K.M., Lei, Z.X. and Zhang, L.W. (2015). Mechanical analysis of functionally graded carbon nanotube reinforced composites: a review", *Compos. Struct.*, **120**, 90-97. https://doi.org/10.1016/j.compstruct.2014.09.041.

Liew, K.M., Lei, Z.X., Yu, J.L. and Zhang, L.W. (2014), "Postbuckling of carbon nanotube-reinforced functionally graded cylindrical panels under axial compression using a meshless approach", *Comput. Meth. Appl. Mech. Eng.*, **268**, 1-17. https://doi.org/10.1016/j.cma.2013.09.001.

Liew, K.M., Pan, Z. and Zhang, L.W. (2020), "The recent progress of functionally graded CNT reinforced composites and structures", *Sci. China Phys. Mech. Astron.*, **63**(3), 234601. https://doi.org/10.1007/s11433-019-1457-2.

Lin, F., Yang, C., Zeng, Q.H and Xiang, Y. (2018), "Morphological and mechanical properties of graphene-reinforced PMMA nanocomposites using a multiscale analysis", *Comput. Mater. Sci.*, **150**, 107-120. https://doi.org/10.1016/j.commatsci.2018.03.048.

Mahmoudi, A., Benyoucef, S., Tounsi, A., Benachour, A., Adda Bedia, E.A. and Mahmoud, S.R. (2019), "A refined quasi-3D shear deformation theory for thermo-mechanical behavior of functionally graded sandwich plates on elastic foundations", *J. Sandw. Struct. Mater.*, **21**(6), 1906-1926. https://doi.org/10.1177/1099636217727577.

Medani, M., Benahmed, A., Zidour, M., Heireche, H., Tounsi, A., Bousahla, A.A., ... & Mahmoud, S.R. (2019), "Static and dynamic behavior of (FG-CNT) reinforced porous sandwich plate", *Steel Compos. Struct.*, **32**(5), 595-610. https://doi.org/10.12989/scs.2019.32.5.595.

Meksi, R., Benyoucef, S., Mahmoudi, A., Tounsi, A., Adda Bedia, E.A. and Mahmoud, S.R. (2019), "An analytical solution for bending, buckling and vibration responses of FGM sandwich plates", *J. Sandw. Struct. Mater.*, **21**(2), 727-757. https://doi.org/10.1177/1099636217698443.

Mirjavadi, S.S., Afshari, B.M., Barati, M.R. and Hamouda, A.M.S. (2019), "Transient response of porous FG nanoplates subjected to various pulse loads based on nonlocal stress-strain gradient theory", *Eur. J. Mech.-A/Solid.*, **74**, 210-220. https://doi.org/10.1016/j.euromechsol.2018.11.004.

Mirjavadi, S.S., Afshari, B.M., Barati, M.R. and Hamouda, A.M.S. (2019), "Nonlinear free and forced vibrations of graphene nanoplatelet reinforced microbeams with geometrical imperfection", *Microsyst. Technol.*, **25**, 3137-3150. https://doi.org/10.1007/s00542-018-4277-4.

Mirjavadi, S.S., Afshari, B.M., Barati, M.R. and Hamouda, A.M.S. (2018), "Strain gradient based dynamic response analysis of heterogeneous cylindrical microshells with porosities under a moving load", *Mater. Res. Exp.*, **6**(3), 035029.

Mirjavadi, S.S., Afshari, B.M., Khezel, M., Shafiei, N., Rabby, S. and Kordnejad, M. (2018), "Nonlinear vibration and buckling of functionally graded porous nanoscaled beams", *J. Brazil. Soc. Mech. Sci. Eng.*, **40**(7), 352. https://doi.org/10.1007/s40430-018-1272-8.

Mirjavadi, S.S., Afshari, B.M., Shafiei, N., Hamouda, A.M.S. and Kazemi, M. (2017), "Thermal vibration of two-dimensional functionally graded (2D-FG) porous Timoshenko nanobeams", *Steel Compos. Struct.*, **25**(4), 415-426. https://doi.org/10.12989/scs.2017.25.4.415.

Mirjavadi, S.S., Forsat, M., Barati, M.R., Abdella, G.M., Afshari, B.M., Hamouda, A.M.S. and Rabby, S. (2019), "Dynamic response of metal foam FG porous cylindrical micro-shells due to moving loads with strain gradient size-dependency", *Eur. Phys. J. Plus*, **134**(5), 214. https://doi.org/10.1140/epjp/i2019-12540-3.

Mirjavadi, S.S., Forsat, M., Barati, M.R., Abdella, G.M., Hamouda, A.M.S., Afshari, B.M. and Rabby, S. (2019), "Post-buckling analysis of piezo-magnetic nanobeams with geometrical imperfection and different piezoelectric contents", *Microsyst. Technol.*, **25**(9), 3477-3488. https://doi.org/10.1007/s00542-018-4241-3.

Mirjavadi, S.S., Forsat, M., Hamouda, A.M.S. and Barati, M.R. (2019), "Dynamic response of functionally graded graphene nanoplatelet reinforced shells with porosity distributions under transverse dynamic loads", *Mater. Res. Exp.*, **6**(7), 075045.

Mirjavadi, S.S., Forsat, M., Nikookar, M., Barati, M.R. and Hamouda, A.M.S. (2019), "Nonlinear forced vibrations of sandwich smart nanobeams with two-phase piezo-magnetic face sheets", *Eur. Phys. J. Plus*, **134**(10), 508. https://doi.org/10.1140/epjp/i2019-12806-8.

Mirjavadi, S.S., Rabby, S., Shafiei, N., Afshari, B.M. and Kazemi, M. (2017), "On size-dependent free vibration and thermal

buckling of axially functionally graded nanobeams in thermal environment", *Appl. Phys. A*, **123**(5), 315. https://doi.org/10.1007/s00339-017-0918-1.

Mohammed, A., Sanjayan, J.G., Nazari, A. and Al-Saadi, N.T.K. (2017), "Effects of graphene oxide in enhancing the performance of concrete exposed to high-temperature", *Austr. J. Civil Eng.*, **15**(1), 61-71. https://doi.org/10.1080/14488353.2017.1372849.

Nieto, A., Bisht, A., Lahiri, D., Zhang, C. and Agarwal, A. (2017), "Graphene reinforced metal and ceramic matrix composites: a review", *Int. Mater. Rev.*, **62**(5), 241-302. https://doi.org/10.1080/09506608.2016.1219481.

Rafiee, M.A., Rafiee, J., Wang, Z., Song, H., Yu, Z.Z. and Koratkar, N. (2009), "Enhanced mechanical properties of nanocomposites at low graphene content", *ACS Nano*, **3**(12), 3884-3890. https://doi.org/10.1021/nn9010472.

Rezaiee-Pajand, M., Masoodi, A.R. and Mokhtari, M. (2018), "Static analysis of functionally graded non-prismatic sandwich beams", *Adv. Comput. Des.*, **3**(2), 165-190. https://doi.org/10.12989/acd.2018.3.2.165.

Sahla, M., Saidi, H., Draiche, K., Bousahla, A.A., Bourada, F. and Tounsi, A. (2019), "Free vibration analysis of angle-ply laminated composite and soft core sandwich plates", *Steel Compos. Struct.*, **33**(5), 663-679. https://doi.org/10.12989/scs.2019.33.5.663.

Semmah, A., Heireche, H., Bousahla, A.A. and Tounsi, A. (2019), "Thermal buckling analysis of SWBNNT on Winkler foundation by non local FSDT", *Adv. Nano Res.*, **7**(2), 89-98. https://doi.org/10.12989/anr.2019.7.2.089.

Shafiei, N., Mirjavadi, S.S., Afshari, B.M., Rabby, S. and Hamouda, A.M.S. (2017), "Nonlinear thermal buckling of axially functionally graded micro and nanobeams", *Compos. Struct.*, **168**, 428-439. https://doi.org/10.1016/j.compstruct.2017.02.048.

Shamsaei, E., de Souza, F.B., Yao, X., Benhelal, E., Akbari, A. and Duan, W. (2018), "Graphene-based nanosheets for stronger and more durable concrete: A review", *Constr. Build. Mater.*, **183**, 642-660. https://doi.org/10.1016/j.conbuildmat.2018.06.201.

She, G.L., Jiang, X.Y. and Karami, B. (2019), "On thermal snap-buckling of FG curved nanobeams", *Mater. Res. Exp.*, **6**(11), 115008. https://doi.org/10.1088/2053-1591/ab44f1.

She, G.L., Yan, K.M., Zhang, Y.L., Liu, H.B. and Ren, Y.R. (2018), "Wave propagation of functionally graded porous nanobeams based on non-local strain gradient theory", *Eur. Phys. J. Plus*, **133**(9), 368. https://doi.org/10.1140/epjp/i2018-12196-5.

Shen, H.S., Xiang, Y., Lin, F. and Hui, D. (2017). Buckling and postbuckling of functionally graded graphene-reinforced composite laminated plates in thermal environments", *Compos. Part B: Eng.*, **119**, 67-78. https://doi.org/10.1016/j.compositesb.2017.03.020.

Song, M., Kitipornchai, S. and Yang, J. (2017), "Free and forced vibrations of functionally graded polymer composite plates reinforced with graphene nanoplatelets", *Compos. Struct.*, **159**, 579-588. https://doi.org/10.1016/j.compstruct.2016.09.070.

Tlidji, Y., Zidour, M., Draiche, K., Safa, A., Bourada, M., Tounsi, A., ... & Mahmoud, S.R. (2019), "Vibration analysis of different material distributions of functionally graded microbeam", *Struct. Eng. Mech.*, **69**(6), 637-649. https://doi.org/10.12989/sem.2019.69.6.637.

Yang, B., Yang, J. and Kitipornchai, S. (2017). Thermoelastic analysis of functionally graded graphene reinforced rectangular plates based on 3D elasticity", *Meccanica*, **52**(10), 2275-2292. https://doi.org/10.1007/s11012-016-0579-8.

Zaoui, F.Z., Ouinas, D. and Tounsi, A. (2019), "New 2D and quasi-3D shear deformation theories for free vibration of functionally graded plates on elastic foundations", *Compos. Part B*, **159**, 231-247. https://doi.org/10.1016/j.compositesb.2018.09.051.

Zarga, D., Tounsi, A., Bousahla, A.A., Bourada, F. and Mahmoud, S.R. (2019), "Thermomechanical bending study for functionally graded sandwich plates using a simple quasi-3D shear deformation theory", *Steel Compos. Struct.*, **32**(3), 389-410. https://doi.org/10.12989/scs.2019.32.3.389.

Zhang, L.W. (2017), "On the study of the effect of in-plane forces on the frequency parameters of CNT-reinforced composite skew plates", *Compos. Struct.*, **160**, 824-837. https://doi.org/10.1016/j.compstruct.2016.10.116.

Zhang, L.W. and Liew, K.M. (2016), "Postbuckling analysis of axially compressed CNT reinforced functionally graded composite plates resting on Pasternak foundations using an element-free approach", *Compos. Struct.*, **138**, 40-51. https://doi.org/10.1016/j.compstruct.2015.11.031.

Zhang, L.W., Liew, K.M. and Reddy, J.N. (2016a), "Postbuckling of carbon nanotube reinforced functionally graded plates with edges elastically restrained against translation and rotation under axial compression", *Comput. Meth. Appl. Mech. Eng.*, **298**, 1-28. https://doi.org/10.1016/j.cma.2015.09.016.

Zhang, L.W., Liew, K.M. and Reddy, J.N. (2016b), "Postbuckling analysis of bi-axially compressed laminated nanocomposite plates using the first-order shear deformation theory", *Compos. Struct.*, **152**, 418-431. https://doi.org/10.1016/j.compstruct.2016.05.040.

Zhang, L.W., Liew, K.M. and Reddy, J.N. (2016c), "Postbuckling behavior of bi-axially compressed arbitrarily straight-sided quadrilateral functionally graded material plates", *Comput. Meth. Appl. Mech. Eng.*, **300**, 593-610. https://doi.org/10.1016/j.cma.2015.11.030.

Zhang, Z., Li, Y., Wu, H., Zhang, H., Wu, H., Jiang, S. and Chai, G. (2020), "Mechanical analysis of functionally graded graphene oxide-reinforced composite beams based on the first-order shear deformation theory", *Mech. Adv. Mater. Struct.*, **27**, 3-11. https://doi.org/10.1080/15376494.2018.1444216.

CC